



UNIVERSITÀ  
DEGLI STUDI  
FIRENZE

FLORE

## Repository istituzionale dell'Università degli Studi di Firenze

### **Membrane cholesterol enrichment prevents Abeta-induced oxidative stress in Alzheimer's fibroblasts.**

Questa è la Versione finale referata (Post print/Accepted manuscript) della seguente pubblicazione:

*Original Citation:*

Membrane cholesterol enrichment prevents Abeta-induced oxidative stress in Alzheimer's fibroblasts / A. Pensalfini ; M. Zampagni ; G. Liguri ; M. Becatti ; E. Evangelisti ; C. Fiorillo ; S. Bagnoli ; E. Cellini ; B. Nacmias ; S. Sorbi ; C. Cecchi. - In: NEUROBIOLOGY OF AGING. - ISSN 0197-4580. - STAMPA. - 32:(2011), pp. 210-222. [10.1016/j.neurobiolaging.2009.02.010]

*Availability:*

This version is available at: 2158/387109 since: 2019-07-25T22:14:15Z

*Published version:*

DOI: 10.1016/j.neurobiolaging.2009.02.010

*Terms of use:*

Open Access

La pubblicazione è resa disponibile sotto le norme e i termini della licenza di deposito, secondo quanto stabilito dalla Policy per l'accesso aperto dell'Università degli Studi di Firenze (<https://www.sba.unifi.it/upload/policy-oa-2016-1.pdf>)

*Publisher copyright claim:*

(Article begins on next page)



# Membrane cholesterol enrichment prevents A $\beta$ -induced oxidative stress in Alzheimer's fibroblasts

Anna Pensalfini<sup>a,1</sup>, Mariagioia Zampagni<sup>a</sup>, Gianfranco Liguri<sup>a,c</sup>, Matteo Becatti<sup>a</sup>,  
Elisa Evangelisti<sup>a</sup>, Claudia Fiorillo<sup>a</sup>, Silvia Bagnoli<sup>b</sup>, Elena Cellini<sup>b</sup>,  
Benedetta Nacmias<sup>b</sup>, Sandro Sorbi<sup>b</sup>, Cristina Cecchi<sup>a,c,\*</sup>

<sup>a</sup> Department of Biochemical Sciences, University of Florence, 50134 Florence, Italy

<sup>b</sup> Department of Neurological and Psychiatric Sciences, University of Florence, 50134 Florence, Italy

<sup>c</sup> Research Centre on the Molecular Basis of Neurodegeneration, University of Florence, 50134 Florence, Italy

Received 29 May 2008; received in revised form 5 February 2009; accepted 9 February 2009

Available online 17 March 2009

## Abstract

A growing body of evidence implicates low membrane cholesterol in the pathogenesis of Alzheimer's disease (AD). Here we show that A $\beta$ 42 soluble oligomers accumulate more slowly and in reduced amount at the plasma membranes of PS-1L392V and APPV717I fibroblasts from familial AD (FAD) patients enriched in cholesterol content than at the counterpart membranes. The A $\beta$ 42-induced production of reactive oxygen species (ROS) and the increase in membrane lipoperoxidation were also prevented by high membrane cholesterol, thus resulting in a higher resistance to amyloid toxicity with respect to control fibroblasts. On the other hand, the recruitment of amyloid assemblies to the plasma membrane of cholesterol-depleted fibroblasts was significantly increased, thus triggering an earlier and sharper production of ROS and a higher membrane oxidative injury. These results identify membrane cholesterol as being key to A $\beta$ 42 oligomer accumulation at the cell surfaces and to the following A $\beta$ 42-induced cell death in AD neurons.

© 2009 Elsevier Inc. All rights reserved.

**Keywords:** Familial Alzheimer's disease; Fibroblasts; APP and PS-1 genes; Membrane cholesterol; Amyloid aggregate toxicity; Oxidative stress

## 1. Introduction

Alzheimer's disease (AD) is a progressive neurodegenerative disorder affecting the elderly that is characterized by irreversible cognitive and physical deterioration. A common feature of AD is the extracellular accumulation of the A $\beta$ 40 and A $\beta$ 42 peptides derived from the proteolytic cleavage of the amyloid precursor protein (APP) carried out by  $\beta$ - and  $\gamma$ -secretase in the amyloidogenic pathway (Selkoe, 2001; Citron et al., 1997; Takeda et al., 2004; Tabaton and

Tamagno, 2007). Evidence for the relationship between the development of AD and abnormal A $\beta$  production also comes from the familial forms of AD (FAD). FAD only accounts for about 5% of all AD cases, but the most significant FAD mutations are all associated with APP processing to yield A $\beta$ . Autosomal dominant forms of FAD are often characterized by specific mutations in the APP gene located on chromosome 21, or in the genes mapped on chromosomes 14 and 1, encoding presenilin-1 (PS-1) and presenilin-2 (PS-2), respectively, which are components of a large protein complex responsible for  $\gamma$ -secretase activity (Cruts and Van Broeckoven, 1998). The amyloid cascade hypothesis causally links AD clinico-pathological process and neuronal cell death to the aggregation and deposition of A $\beta$  (Selkoe, 2001). Nevertheless, a recently modified "amyloid cascade hypothesis" for AD indicates that prefibrillar A $\beta$ 40 and A $\beta$ 42 oligomers, also known as amyloid  $\beta$ -derived diffusible ligands (ADDLs),

\* Corresponding author at: Department of Biochemical Sciences, University of Florence, Viale Morgagni 50, 50134 Florence, Italy.  
Tel.: +39 055 4598320; fax: +39 055 4598905.

E-mail address: [cristina.cecchi@unifi.it](mailto:cristina.cecchi@unifi.it) (C. Cecchi).

<sup>1</sup> Present address: Department of Molecular Biology and Biochemistry, University of California, Irvine, CA 92697, USA.

are the main responsible of cytotoxicity and synapse failure (Klein, 2002; Lacor et al., 2004).

A leading theory on the molecular basis of amyloid toxicity suggests that amyloid unstable assemblies interact with cell membranes destroying their ordered structure, eventually leading to membrane permeabilization with subsequent alteration of ion homeostasis and intracellular redox status (Bokvist et al., 2004; Kaye et al., 2004; Stefani and Dobson, 2003). Indeed we have recently described that amyloid oligomers exogenously added to the culture medium of FAD fibroblasts can readily insert into oxidative-damaged APPV717I fibroblasts where the membrane integrity is compromised, resulting in a prompt increase in the production of reactive oxygen species (ROS) (Cecchi et al., 2007). These data support the rising consensus on the role of membranes as initial triggers of the biochemical modifications culminating with cell death (Wakabayashi et al., 2005).

Recent studies have described a key role for membrane cholesterol in modulating A $\beta$  peptide production, clearance, aggregation and neurotoxicity (Abad-Rodriguez et al., 2004; Mazziotti and Perlmutter, 1998; Ledesma and Dotti, 2006; Zhou and Richardson, 1996; Yip et al., 2001; Arispe and Doh, 2002; Kawahara and Kuroda, 2001; Sponne et al., 2004). The presence of cholesterol in neuronal membranes is known to induce large changes in membrane physical features such as fluidity and density of lipid packing resulting in alterations of aggregate recruitment to the membrane and membrane permeabilization (Arispe and Doh, 2002; Mirzabekov et al., 1996). In particular, it has been reported that the presence of cholesterol in artificial lipid bilayers inhibits the channel-forming activity of human amylin, A $\beta$ 40, A $\beta$ 42, and A $\beta$ 25–35 peptides (Arispe and Doh, 2002; Chochina et al., 2001; Mirzabekov et al., 1996; Lin and Kagan, 2002). Membrane cholesterol also interferes with neuronal apoptosis induced by soluble oligomers of A $\beta$  peptide (Sponne et al., 2004). On the other hand, reducing membrane cholesterol makes the cell more vulnerable to the action of amyloid aggregates (Arispe and Doh, 2002). Accordingly, we previously reported a significant correlation between resistance to amyloid toxicity and membrane cholesterol content in various cultured cell types (Cecchi et al., 2005).

It has recently been shown that seladin-1 gene, whose proteic product catalyzes the last steps of cholesterol biosynthesis (Waterham et al., 2001), appears to be down-regulated in brain areas affected by AD (Greeve et al., 2000). Our recent findings also indicate that seladin-1-induced membrane cholesterol enrichment protects SH-SY5Y cells against amyloid toxicity by reducing the interaction of A $\beta$ 42 oligomer with cell membrane, featuring seladin-1 as a susceptibility gene candidate for sporadic AD (Cecchi et al., 2008).

Here we carried out a study on cultured skin fibroblasts from FAD patients bearing either APP or PS-1 gene mutations, and age-matched healthy control cells with increased or diminished membrane cholesterol levels by cell culture media supplementation with water soluble cholesterol (PEG-

cholesterol) or methyl- $\beta$ -cyclodextrin ( $\beta$ -CD), respectively. Under these conditions we investigated the dependence of cell vulnerability to A $\beta$ 42 aggregates on membrane cholesterol content, by checking the extent of amyloid aggregate interaction with the cell membrane, oxidative stress and cell death markers in FAD fibroblasts compared to healthy cells. We found that (i) membrane cholesterol enrichment significantly reduces the interaction of A $\beta$ 42 oligomers with the cell membrane of FAD fibroblasts; on the other hand, amyloid aggregate interaction was significantly increased in fibroblasts with reduced membrane cholesterol levels; (ii) membrane cholesterol enrichment significantly prevents intracellular ROS production and membrane lipoperoxidation with respect to cholesterol-depleted cells; (iii) the higher resistance to amyloid-induced oxidative stress in cholesterol-enriched fibroblasts matched an improved cell viability. Although a direct link between alterations in the homeostasis of membrane cholesterol and AD pathogenesis is far from been clear, our results support the idea that neuronal resistance to A $\beta$  toxicity requires the maintenance of a proper steady-state level of membrane cholesterol.

## 2. Materials and methods

### 2.1. Materials

All reagents were of analytical grade or the highest purity available. Congo Red, fetal bovine serum (FBS),  $\beta$ -CD, polyoxyetanyl-cholesteryl sebacate (PEG-chol), vitamin E, filipin III and other chemicals were from Sigma (Milan, Italy) unless otherwise stated. 2',7'-dichlorodihydrofluorescein diacetate, acetyl ester (CM-H<sub>2</sub>DCFDA), 4,4-difluoro-3a,4adiazas-indacene (BODIPY 581/591 C<sub>11</sub>), wheat germ agglutinin conjugated with fluorescein or with Alexa Fluor 633 and pluronic acid F127 were from Molecular Probes (Eugene, OR). CM-H<sub>2</sub>DCFDA and BODIPY 581/591 C<sub>11</sub> were prepared as stock solutions in dimethylsulfoxide (DMSO), purged with nitrogen and stored in light-protected vessels at  $-20^{\circ}\text{C}$  until use. A $\beta$ 42 and A $\beta$ 42-1 peptides, as trifluoroacetate salts, were purchased from Bachem (Bubendorf, Switzerland), A $\beta$ 42 amine-reactive succinimidyl esters of carboxyfluorescein (A $\beta$ 42-FAM) was from AnaSpec (Simakova and Arispe, 2007). Lyophilized A $\beta$ 42, A $\beta$ 42-FAM and A $\beta$ 42-1 were initially incubated in 1 mM in hexafluoro-2-propanol (HFIP) at least for 1 h at room temperature to allow complete peptide monomerization (Lambert et al., 2001). Then, aliquots of peptide solutions were dried under nitrogen and stored at  $-80^{\circ}\text{C}$ . Lyophilized amylin 1–37 (Sigma, Milan, Italy) was stored and processed as previously reported (Cecchi et al., 2005).

### 2.2. Cell culture and treatment

In the present study we investigated nine fibroblast cell lines. Fibroblasts were obtained from three patients

belonging to Italian families bearing the APP Val717Ile mutation (mean  $\pm$  SD age =  $53.3 \pm 7.1$  years) and from three patients belonging to other Italian families bearing the PS-1 Leu392Val and Met146Leu mutations (mean  $\pm$  SD age =  $56.7 \pm 8.6$  years), respectively. They underwent clinical assessment according to published guidelines and the AD diagnosis fulfilled the Diagnostic and Statistical Manual of Mental Disorders criteria (DSM-IV) (American Psychiatric Association, 1994; The Dementia Study Group of the Italian Neurological Society, 2000). Three age-matched healthy subjects (mean  $\pm$  SD age =  $49.7 \pm 8.3$  years) were also analyzed. The local ethical committee approved the protocol of the study and written consent was obtained from all subjects or, where appropriate, their caregivers. All control subjects were tested and none of them carried APP or PS-1 mutations. These subjects were also carefully assessed with a rigorous diagnostic evaluation in order to exclude diagnosis of other neurological disorders. Skin biopsies of 3 mm punch were obtained from the volar side of the upper arm of the FAD patients and healthy controls. The cells were grown in Dulbecco's modified Eagle's medium (DMEM), supplemented with 10% FBS, and harvested at confluence in T-25 flasks, 7 days after previous subculture (Cecchi et al., 2007). All fibroblast lines were subjected to an equal number of passages (ranging from 10 to 18) and analyzed in three different experiments before confluence. Human SH-SY5Y neuroblastoma cells (ATCC, Manassas, VA) were cultured in DMEM F-12 Ham with 25 mM HEPES and  $\text{NaHCO}_3$  (1:1) supplemented with 10% FBS, 1.0 mM glutamine and antibiotics in a 5.0%  $\text{CO}_2$  humidified atmosphere at  $37^\circ\text{C}$  and grown until 80% confluence. The increase in membrane cholesterol content was achieved by supplementing fibroblast culture media with 0.5 mM PEG-cholesterol for 2 h and neuroblastoma cell culture media with 0.1 mM PEG-cholesterol for 1 h at  $37^\circ\text{C}$ . Membrane cholesterol depletion was performed by incubating fibroblasts with 1.0 mM  $\beta$ -CD for 2 h and neuroblastoma cells with 1.0 mM  $\beta$ -CD for 30 min at  $37^\circ\text{C}$  in the presence of 1% FBS. Then cells were extensively washed with phosphate buffered saline (PBS) and exposed to 1.0  $\mu\text{M}$  A $\beta$ 42 soluble oligomers obtained according to Lambert's protocol (Lambert et al., 2001). In an other set of experiments, APP fibroblasts were treated with 5.0  $\mu\text{M}$  fluorescein-labeled A $\beta$ 42-FAM aggregates obtained by Lambert's protocol performed on a mixture of A $\beta$ 42-FAM peptide with 2 molar equivalents of unlabeled A $\beta$ 42 peptide (at ratio of 1:2) to minimize possible interference of the fluorophore with the aggregation while retaining sufficient fluorescent signal. For fibrillar conditions, 10 mM HCl was added to bring the peptide to a final concentration of 100  $\mu\text{M}$ , and the peptide was incubated for 24 h at  $37^\circ\text{C}$  (Dahlgren et al., 2002). Western blotting analysis of A $\beta$ 42 soluble oligomers was performed on a Criterion XT Precast gel 4–12% Bis-Tris SDS/PAGE (Bio-Rad, Milan Italy), blotted onto a PVDF Immobilon-P Transfer Membrane (Millipore Corporation, Bedford, MA). The membrane was blocked in 1.0% (w/v) BSA in TBS-Tween (0.1% Tween

20 in 20 mM Tris-HCl, pH 7.5, containing 100 mM NaCl) and incubated with 1:1000 diluted mouse monoclonal 6E10 anti-A $\beta$  antibodies (Signet, Dedham, MA) and then with 1:5000 diluted peroxidase-conjugated anti-mouse secondary antibodies (Pierce, Rockford, IL, USA). The immunolabeled bands were detected using a SuperSignal West Dura (Pierce, Rockford, IL, USA).

### 2.3. Membrane cholesterol assay

The labeling of membrane cholesterol was investigated by confocal scanning microscopy analysis, using the fluorescent probe filipin. Briefly, the cells seeded on glass coverslips were fixed in 4.0% buffered paraformaldehyde for 20 min at  $0^\circ\text{C}$  and then were incubated with 0.25 mg/ml cholesterol-binding agent in PBS for 24 h at  $37^\circ\text{C}$ . After washing, the cells were fixed again in 4.0% buffered paraformaldehyde for 20 min at  $0^\circ\text{C}$ . Cell fluorescence was analyzed by a confocal Leica TCS SP5 scanning microscope (Mannheim, Germany) equipped with an argon laser source for fluorescence measurements using emission lines at 510 nm for filipin excitation.

Cholesterol content was assayed in membrane fractions using the sensitive fluorimetric Amplex Red Cholesterol Assay Kit (Molecular Probes, Eugene, OR), by comparison with a reference curve of cholesterol (0.01–1  $\mu\text{g}$ ) (Amundson and Zhou, 1999). Membrane fractions were obtained as previously described, with minor modifications (Cecchi et al., 2008). Briefly, cells were washed twice in PBS and dissolved in PBS containing 9.0% sucrose, 0.1 mM phenylmethylsulphonylfluoride (PMSF), 10  $\mu\text{g}/\text{ml}$  leupeptin and 10  $\mu\text{g}/\text{ml}$  aprotinin prior to storage at  $-80^\circ\text{C}$  until use. Then, cells were homogenized in PBS containing 9.0% sucrose with three freeze-thaw cycles, 5 s sonication in ice. The samples were centrifuged at  $700 \times g$  for 10 min at  $4^\circ\text{C}$  and a further centrifugation of the supernatant was performed at  $110,000 \times g$  for 1 h at  $4^\circ\text{C}$  to pellet the membrane fraction. Protein content in the membrane fractions was measured by the method of Bradford (1976).

### 2.4. Time-course of aggregate binding to the cell membrane

The interaction of A $\beta$ 42 aggregates with plasma membranes was monitored in FAD, healthy fibroblasts and SH-SY5Y neuroblastoma cells seeded on glass coverslips by confocal scanning microscopy as previously described (Cecchi et al., 2007, 2008). Briefly, after treatment with 1.0  $\mu\text{M}$  A $\beta$ 42 prefibrillar aggregates for 30, 60, and 180 min, the cells were counterstained with fluorescein-conjugated wheat germ agglutinin (50  $\mu\text{g}/\text{ml}$ ) for 10 min to detect plasma membrane profiles and fixed in 2% buffered paraformaldehyde for 10 min at room temperature. After plasma membrane permeabilization with a 3% glycerol solution, the coverslips were incubated for 60 min with 1:1000 diluted mouse monoclonal 6E10 anti-A $\beta$  antibodies and then with 1:1000 diluted Texas



Red-conjugated anti-mouse secondary antibodies (Vector Laboratories, DBA, Italy) for 90 min. Aggregate adsorption to the fibroblasts was also analyzed by cell treatment with 5.0  $\mu$ M A $\beta$ 42-FAM oligomers, counterstain of plasma membranes with Alexa Fluor 633-conjugated wheat germ agglutinin and fixing in 2% buffered paraformaldehyde, without plasma membrane permeabilization or using antibodies. The fluorescence was analyzed by a confocal Leica TCS SP5 scanning microscope (Mannheim, Germany) equipped with an argon laser source for fluorescence measurements using two emission lines at 568 nm and 488 nm for Texas Red and fluorescein excitation, respectively. A series of optical sections (1024  $\times$  1024 pixels) 1.0  $\mu$ m in thickness was taken through the cell depth at intervals of 0.5  $\mu$ m using a Leica Plan Apo 63  $\times$  oil immersion objective and then projected as a single composite image by superimposition. The quantitation of aggregate adsorption to the cell surface of FAD and healthy fibroblasts was performed using the specific Congo Red dye as previously described (Cecchi et al., 2007). Briefly, the same number of cells was treated for 10, 20, 30 and 60 min with 1.0  $\mu$ M A $\beta$ 42 aggregates in a 96-well plate and then washed twice with PBS. The residual aggregate-cell complex was stained with 100  $\mu$ l of 1.0  $\mu$ M Congo Red in PBS for 20 min at 37  $^{\circ}$ C and measured photometrically at 550 nm with an ELISA plate reader according to Datki et al. (2004). Congo Red values are reported as percent increases with respect to untreated fibroblasts (assumed as 100%). For flow cytometric analysis of A $\beta$ 42 binding, APP fibroblasts were incubated in the cell culture medium containing 5.0  $\mu$ M A $\beta$ 42-FAM aggregates, obtained as above reported, for 60 min and then analyzed by a FACSCanto (Beckton Dickinson Biosciences, San Jose, CA).

### 2.5. Evaluation of ROS production and intracellular ROS scavengers

FAD and healthy fibroblasts, representative of cholesterol enrichment or depletion conditions, were cultured on glass coverslips and exposed to 1.0  $\mu$ M A $\beta$ 42 aggregates for 30, 60, and 180 min. As a negative control for oxidative stress, fibroblasts were pre-treated with 100  $\mu$ M vitamin E for 24 h at 37  $^{\circ}$ C, before membrane cholesterol modulation and aggregate exposure. Dye loading was achieved by adding to the cell culture media 5.0  $\mu$ M ROS-sensitive fluorescent probe CM-H<sub>2</sub>DCFDA dissolved in 0.1% DMSO and pluronic acid F-127 (0.01%, w/v) for 10 min at 37  $^{\circ}$ C. Then, the cells were fixed and the emitted CM-H<sub>2</sub>DCFDA fluorescence was detected at 488-nm excitation by a Leica Plan Apo 63  $\times$  oil immersion objective.

Intracellular hydrophilic ROS scavengers were measured in cell lysates, obtained as previously reported (Cecchi et al., 2005), of FAD and healthy fibroblasts exposed to 1.0  $\mu$ M A $\beta$ 42 aggregates for 3 h, by a chemiluminescence assay using the photoprotein Pholasin (Abel Antioxidant Test Kit, Knight Scientific Limited, UK). The results were calculated using an L-ascorbic acid-based standard curve.

### 2.6. Analysis of lipoperoxidation

To assess the rate of lipid peroxidation, isoprostane levels were measured photometrically at 405 nm in the cell lysates using the 8-isoprostane EIA kit (Cayman Chemical Company, Ann Arbor, MI) following the manufacturer's instructions. Lipid peroxidation after cell aggregate exposure was also investigated by confocal scanning microscopy analysis, using the fluorescent probe BODIPY 581/591 C<sub>11</sub>, as previously described (Pensalfini et al., 2008). In particular, BODIPY 581/591 C<sub>11</sub> by mimicking the properties of natural lipids (Naguib, 1998) can be used to measure antioxidant activity in lipid environments since it behaves as a fluorescent lipid peroxidation reporter that shifts its fluorescence from red to green when challenged with oxidizing agents (Drummen et al., 2004). Briefly, fibroblasts, representative of cholesterol enrichment or depletion conditions, were cultured on glass coverslips and exposed 1.0  $\mu$ M A $\beta$ 42 aggregates for 3 h at 37  $^{\circ}$ C. As a negative control, fibroblasts were pre-treated with 100  $\mu$ M vitamin E for 24 h at 37  $^{\circ}$ C, before membrane cholesterol modulation and aggregate exposure. Dye loading was achieved by adding to the cell culture media the fluorescent probe BODIPY dissolved in 0.1% DMSO (5.0  $\mu$ M final concentration) for 30 min at 37  $^{\circ}$ C. The cells were fixed in 2% buffered paraformaldehyde for 10 min at room temperature and the BODIPY fluorescence was detected at 581-nm excitation by collecting the emitted fluorescence with a Leica Plan Apo 63  $\times$  oil immersion objective as above reported.

### 2.7. Amyloid cytotoxicity assay

Aggregate cytotoxicity to FAD and healthy fibroblasts was assessed in 96-well plates by the 3-(4,5-dimethylthiazol-2-yl)-2,5-diphenyltetrazolium bromide (MTT) assay as previously reported (Cecchi et al., 2007). Briefly, after the exposure to 1.0  $\mu$ M A $\beta$ 42 monomers, oligomers or fibrils or to A $\beta$ 42-1 reversed sequence peptide or amylin for 24 h at 37  $^{\circ}$ C, the cell cultures were incubated with 0.5 mg/ml MTT solution at 37  $^{\circ}$ C for 4.0 h and with cell lysis buffer (20% SDS, 50% N,N-dimethylformamide, pH 4.7) overnight. As a negative control for oxidative stress, fibroblasts were pre-treated with 100  $\mu$ M vitamin E for 24 h at 37  $^{\circ}$ C, before membrane cholesterol modulation and aggregate exposure. Absorbance values of blue formazan were determined at 590 nm using an ELISA plate reader. Cell viability was expressed as percent of MTT reduction in treated cells as compared to counterpart untreated cells, where it was assumed as 100%. Moreover, the effect of aggregate treatments on cell morphology was investigated by Hoechst 33342 dye staining. Briefly, fibroblasts treated as above reported were incubated with 20  $\mu$ g/ml Hoechst for 15 min at 37  $^{\circ}$ C and fixed 2% buffered paraformaldehyde for 10 min at room temperature. Blue fluorescence micrographs of cells were obtained under UV illumination in an epifluorescence inverted microscope (Nikon, Diaphot TMD-EF) with an appropriate filter set.

Finally, lactate dehydrogenase (LDH) release into the culture media, a typical necrotic marker, was measured after cell exposure to 1.0  $\mu$ M A $\beta$ 42 aggregates or to A $\beta$ 42-1 reversed sequence peptide for 48 h at 37 °C by the LDH assay kit (Roche Diagnostics, Mannheim, Germany) at 490 nm after blank subtraction at 595 nm.

### 2.8. Statistical analysis

All data were expressed as mean values  $\pm$  standard deviation (SD). The comparisons among the different groups were performed by ANOVA followed by Bonferroni's *t*-test. A *p*-value less than 0.05 was accepted as statistically significant.

## 3. Results

### 3.1. Membrane cholesterol enrichment reduces A $\beta$ aggregate binding to the cell membrane

Cell degeneration in amyloid diseases appears to be mediated by a toxic mechanism involving some interaction of the aggregated species with the plasma membrane of the affected cells (Bokvist et al., 2004; Kaye et al., 2004; Stefani and Dobson, 2003). We previously showed that A $\beta$ 42 aggregates accumulate quicker near the plasma membrane in FAD fibroblasts than in wild-type cells possibly as a result of increased membrane lipoperoxidation (Cecchi et al., 2007). Here, we investigated the dependence of the membrane-binding capacity of A $\beta$ 42 soluble oligomers (Fig. 1a) on membrane cholesterol content in PS-1, APP and wild-type fibroblasts. In particular, we induced modifications of membrane cholesterol content by incubating FAD and healthy fibroblasts in the presence of either PEG-cholesterol or  $\beta$ -

CD followed by extensive washing with PBS. As shown in Fig. 1b, a morphological evaluation of FAD and healthy fibroblasts by confocal microscopy revealed a clear modulation of membrane cholesterol content under our experimental conditions. Quantitative analysis confirmed that cell exposure to soluble cholesterol resulted in a significant increase in membrane cholesterol (about 20%) vs respective control cells in all investigated fibroblast lines (Fig. 1b). Conversely, fibroblasts treated with  $\beta$ -CD underwent a significant reduction in membrane cholesterol (about 25%) vs counterpart fibroblasts. The increase in plasma membrane cholesterol resulted in a reduced amyloid-binding capacity to the plasma membrane of FAD fibroblasts with respect to relative cells, as assessed by confocal microscopy analysis of cells exposed for 30, 60 and 180 min to A $\beta$ 42 aggregates (Fig. 2a). Accordingly, the Congo Red assay showed that cell media supplementation with soluble cholesterol resulted in a significant reduction of A $\beta$ 42 aggregate binding to the cell plasma membranes with respect to controls (Fig. 2b). On the other hand, in fibroblasts from healthy subjects just few aggregates following longer time of protein exposure can be observed (Fig. 2a). Conversely, the same amyloid oligomers added to the cell culture medium appear to accumulate more rapidly and to a greater extent at the plasma membrane in  $\beta$ -CD treated cells characterized by a reduced content of cholesterol than in counterpart cells (Fig. 2a and b). Furthermore, A $\beta$ 42 assemblies share a more rapid kinetic of interaction with cell surfaces in APP than in PS-1 fibroblasts. No significant difference in Congo Red absorbance values between wild-type and FAD groups of A $\beta$ 42-untreated cells was observed. An equal cell number from cultures with a comparable division rate from different donors were exposed to the aggregates in order to exclude the influence of these factors on the amount of A $\beta$  bounded to the cell surface. The ability of exposed cells

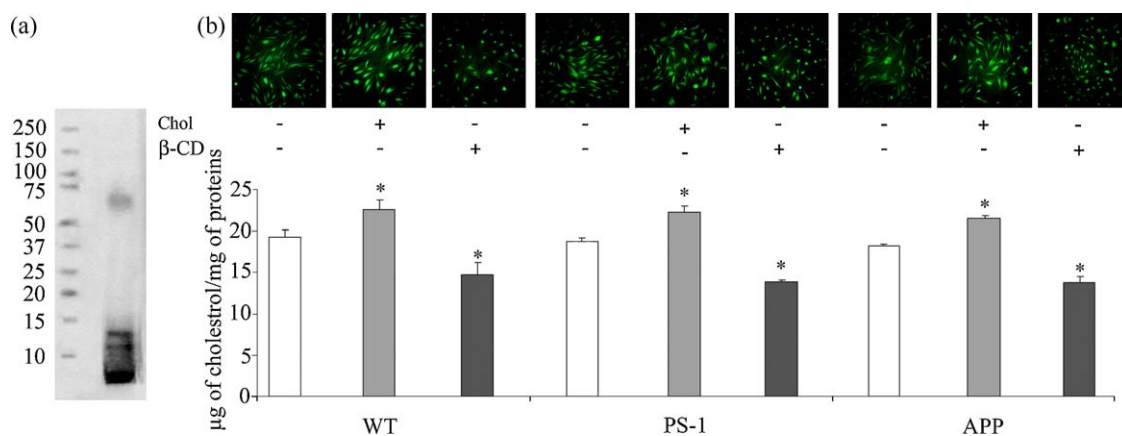


Fig. 1. Modulation of membrane cholesterol in FAD and healthy fibroblasts. (a) Representative Western blotting analysis of A $\beta$ 42 soluble oligomers separated by SDS/PAGE on a 4–12% criterion XT Precast Bis–Tris gel and probed with monoclonal mouse 6E10 antibodies and with peroxidase-conjugated anti-mouse antibodies. (b) Representative confocal microscopy analysis of membrane cholesterol in WT, PS-1 and APP fibroblasts probed by the fluorescent dye filipin. Membrane cholesterol enrichment was achieved by incubating WT, PS-1 and APP fibroblasts with 0.5 mM PEG-cholesterol (Chol) for 2 h at 37 °C; membrane cholesterol depletion was performed by adding 1.0 mM  $\beta$ -CD for 2 h at 37 °C in the culture media. The amount of cholesterol was determined using cholesterol oxidase, as described in Section 2. The reported values are representative of three independent experiments. \*Significant difference ( $p \leq 0.05$ ) vs relative control cells with basal cholesterol levels.

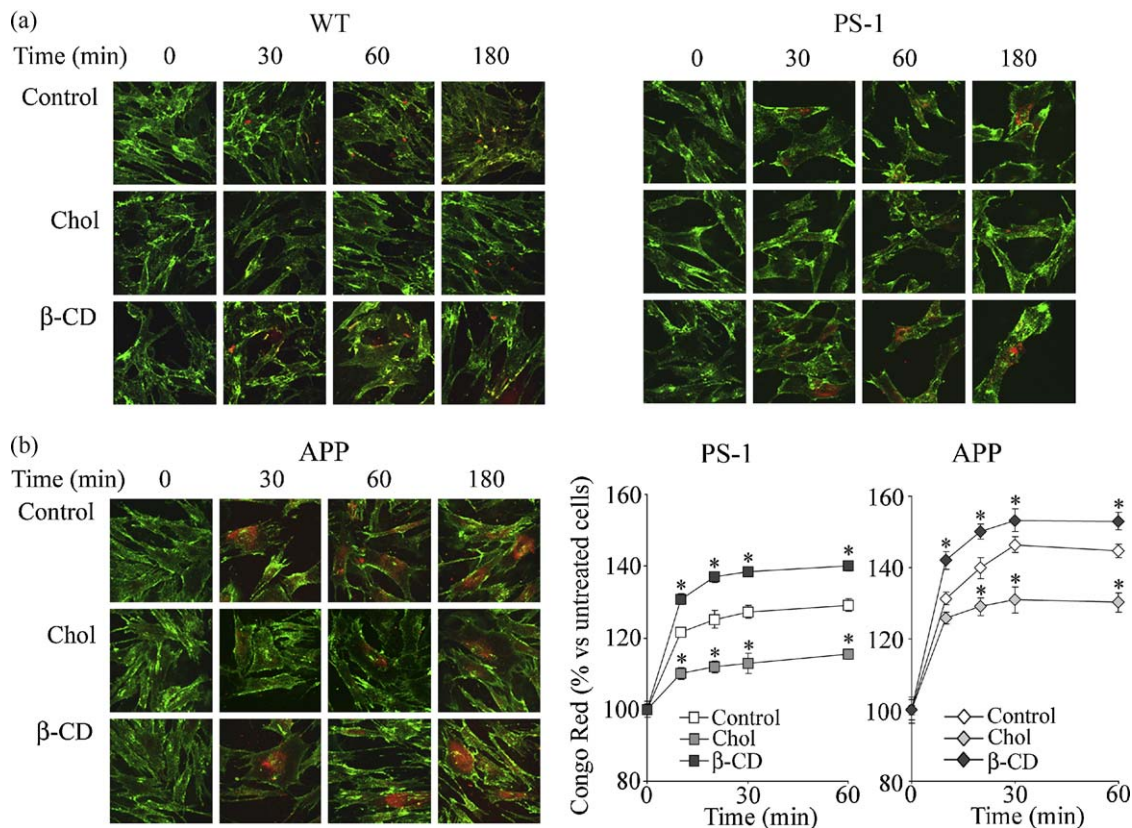


Fig. 2. Increasing cell cholesterol reduces A $\beta$  aggregate binding to the cell membrane. (a) Confocal microscopy images show aggregates penetrating into the plasma membrane of wild-type, PS-1 and APP fibroblasts under different experimental conditions. After treatment for 0, 30, 60 and 180 min with 1.0  $\mu$ M A $\beta$ 42 aggregates, counterstaining was performed with fluorescein-conjugated wheat germ agglutinin to detect plasma membrane profile (green). The aggregates were labeled with monoclonal mouse 6E10 anti-A $\beta$  antibodies and Texas Red-conjugated anti-mouse secondary antibodies with plasma membrane permeabilization with glycerol, as specified in Section 2. (b) Time-course of amyloid aggregate binding to PS-1 and APP fibroblasts. After the exposure to 1.0  $\mu$ M A $\beta$ 42 aggregates for 0, 10, 20, 30, 60 min, cells were washed and the residual aggregate-cell complex was stained with 1.0  $\mu$ M Congo Red for 20 min. Under these conditions, Congo Red-staining is a measure of the amount of A $\beta$ 42 aggregates adsorbed to cell membrane surface. The reported values (means  $\pm$  SD) are representative of three independent experiments each carried out in triplicate. \*Significant difference ( $p \leq 0.05$ ) vs relative control cells with basal cholesterol levels. (For interpretation of the references to color in this figure legend, the reader is referred to the web version of the article.)

to bind A $\beta$  aggregates appeared saturable, reaching its limit in the first 30–60 min (Fig. 2b). Moreover, the red fluorescence signals related to 6E10 antibody, that recognizes also the full length human APP, are negligible in all the analyzed conditions before A $\beta$  treatment (see time 0). This evidence let us to rule out the possibility that the differences in the accumulation of exogenous A $\beta$  at the cell surface were due to different levels of APP expression or to the presence of APP mutant forms in these cells. In order to exclude the contribute of intracellular A $\beta$  to 6E10 red signals, a set of experiments was carried out in the same experimental conditions with fluorescein-labeled A $\beta$ 42-FAM aggregates. Confocal microscopy images of fibroblasts treated with A $\beta$ 42-FAM aggregates also confirmed the idea that the ability of A $\beta$ 42 aggregates to bind to the plasma membrane is significantly affected by its content in cholesterol (Fig. 3a). The staining profile of APP fibroblasts exposed to A $\beta$ 42-FAM aggregates retained a less fluorescent signal compared to images shown in Fig. 2a, since to minimize fluorophore interference with the aggregation process, the oligomers were prepared by mix-

ing just one A $\beta$ 42-labeled molecule with two equivalents of A $\beta$ 42-unlabeled peptide. Amyloid binding to APP fibroblasts, as a function of membrane cholesterol content, was also quantified by flow cytometric analysis. Histograms illustrating the distribution for A $\beta$ 42-FAM-positive fibroblasts are shown in Fig. 3b. A higher percentage of fluorescent-positive cells (+42%) in fibroblasts with low membrane cholesterol with respect to controls was evident, as indicated by the shift of the distribution curve toward higher intensity levels. On the other hand, the increase in membrane cholesterol resulted in a lower percentage of fibroblasts (–39%) with surface-binding affinity toward fluorescent A $\beta$ 42-FAM aggregates.

To make these data more relevant, we extended our study to human SH-SY5Y neuroblastoma cells in basal condition ( $10.84 \pm 0.54 \mu$ g membrane cholesterol/mg of protein), in cells significantly enriched in cholesterol content ( $13.55 \pm 0.68 \mu$ g membrane cholesterol/mg of protein;  $p \leq 0.01$ ) and in cells significantly depleted in cholesterol content ( $8.26 \pm 0.73 \mu$ g membrane cholesterol/mg of



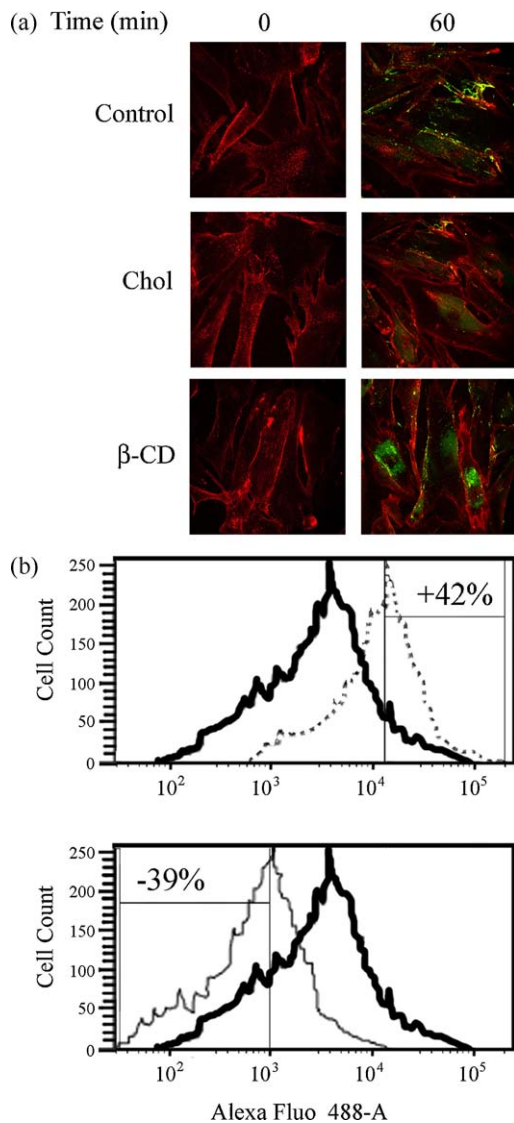


Fig. 3. A $\beta$  aggregate binding inversely correlates with membrane cholesterol content. (a) Confocal microscopy images show fluorescein-labeled A $\beta$ 42-FAM aggregates (green) penetrating into the plasma membrane of APP fibroblasts with different membrane cholesterol content. Membrane profile was counterstained with Alexa Fluor 633-conjugated wheat germ agglutinin (red). (b) Flow cytometry analysis of A $\beta$ 42-FAM binding to APP fibroblasts after treatment for 60 min with 1.0  $\mu$ M A $\beta$ 42 aggregates in basal (solid line), in cholesterol-depleted (dotted line) and in cholesterol-enriched conditions (thinner solid line) (see Section 2 for details). Histograms of the number of cells vs A $\beta$ 42-FAM fluorescence. Fluorescent gates were used to separate cells with lower A $\beta$ 42-FAM binding affinity and cells with higher A $\beta$ 42-FAM binding affinity with respect to control cells. (For interpretation of the references to color in this figure legend, the reader is referred to the web version of the article.)

protein;  $p \leq 0.01$ ). According to fibroblast data, the increase in plasma membrane cholesterol resulted in a reduced A $\beta$  oligomer binding to the plasma membrane in human neuroblastoma cells as detected by confocal microscopy analysis using monoclonal anti-A $\beta$  antibodies (Fig. 4). On the other hand, the same oligomers added to the neuroblastoma culture medium appeared to accumulate to a greater extent at

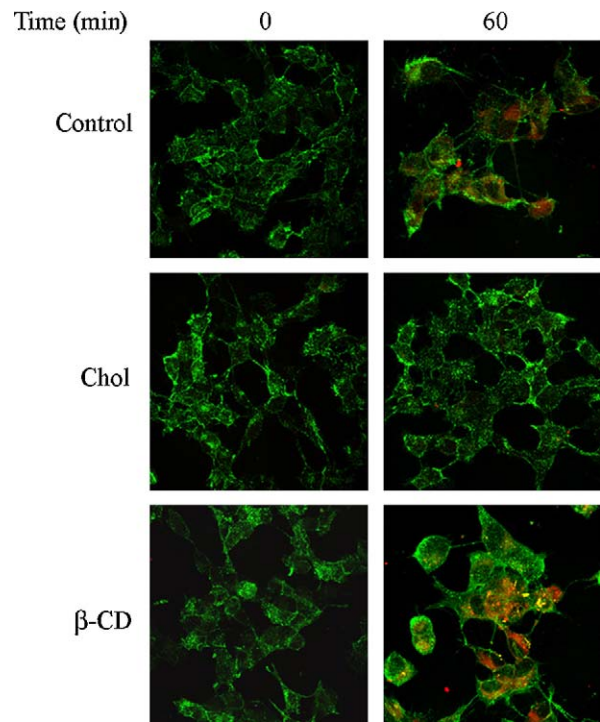


Fig. 4. Membrane cholesterol modulates A $\beta$  aggregate binding to human SH-SY5Y neuroblastoma cells. Representative confocal microscopy images showing aggregates penetrating into the plasma membrane of neuroblastoma cells after cell treatment for 0 or 1 h with 1.0  $\mu$ M A $\beta$ 42 aggregates in basal conditions, in cholesterol enriched cells (Chol) and in cholesterol-depleted cells ( $\beta$ -CD) (see Section 2 for details).

the plasma membrane in  $\beta$ -CD treated cells characterized by reduced membrane cholesterol content.

### 3.2. Membrane cholesterol enrichment reduces ROS production and ROS scavenger impairment

There is strong experimental evidence that oxidative stress is an early biochemical modification in cells facing amyloid aggregates (Butterfield et al., 2007). Therefore, we investigated the dependence of ROS production on membrane cholesterol content in human fibroblasts exposed to amyloid aggregates. A time-course analysis showed that in APP and, to a lesser extent, in PS-1 fibroblasts an earlier and sharper increase in intracellular ROS content than in wild-type fibroblasts (Fig. 5a). The reduced ability of APP cells to counteract A $\beta$ 42 aggregate oxidative attack was also confirmed by a significant impairment in intracellular ROS scavengers with respect to that observed in PS-1 and wild-type fibroblasts. Indeed, ROS scavengers were significantly different among the investigated fibroblast lines with basal cholesterol content ( $1500 \pm 52$  nmol ascorbate/mg of proteins in wild-type,  $1170 \pm 39$  nmol ascorbate/mg of proteins in PS-1, and of  $821 \pm 49$  nmol ascorbate/mg of proteins in APP fibroblasts), according to our previous reported data (Cecchi et al., 2002). Interestingly, PEG-cholesterol addition to the cell culture media was as effective as vitamin



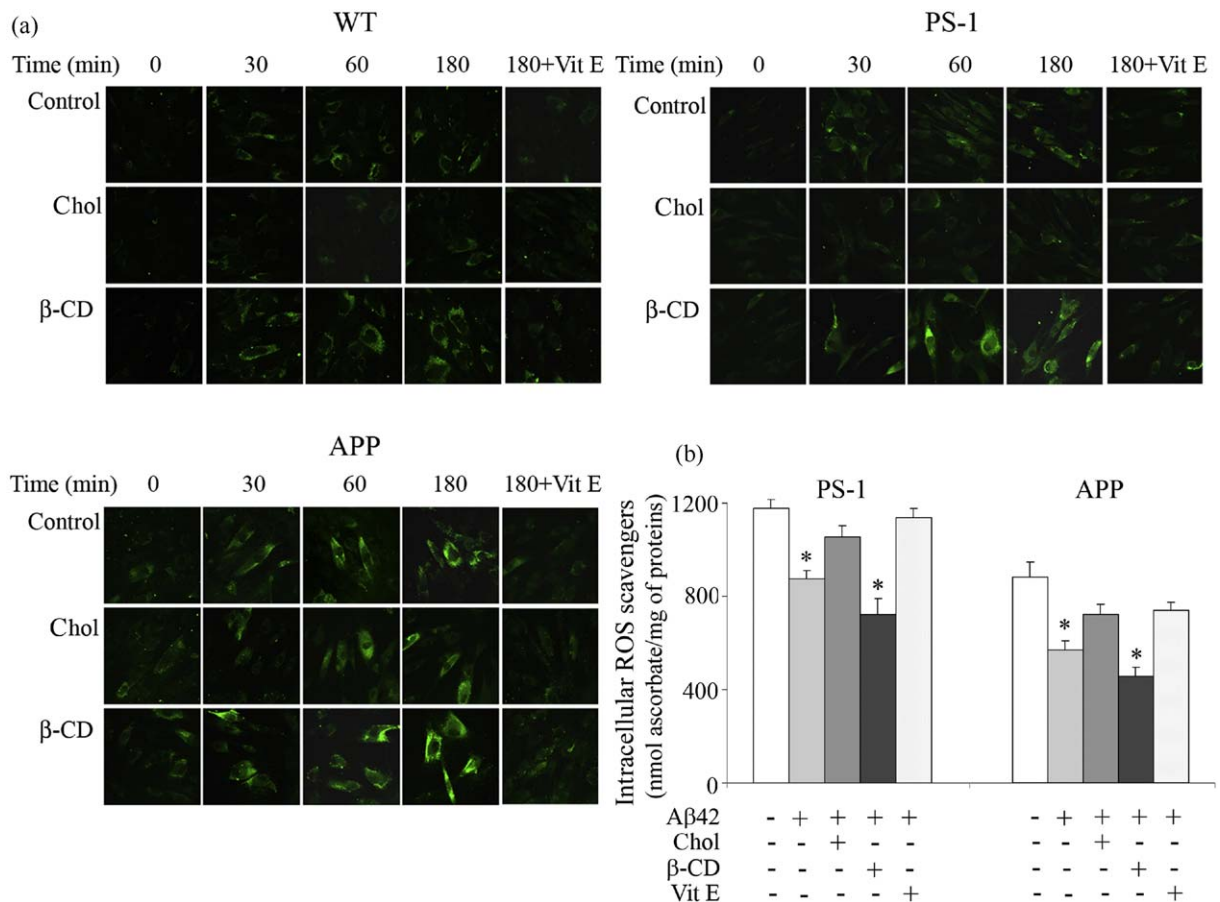


Fig. 5. Cholesterol enrichment reduces A $\beta$ 42-induced ROS production and ROS scavenger weakening. (a) Representative confocal images of intracellular ROS levels in WT, PS-1 and APP fibroblasts under different experimental conditions. After treatment for 0, 30, 60 and 180 min with 1.0  $\mu$ M A $\beta$ 42 prefibrillar aggregates, cells were incubated for 10 min in the presence of the redox fluorescent probe CM-H<sub>2</sub>DCFDA and then fixed. Vitamin E (Vit E) was used as negative control. For details see Section 2. (b) Intracellular ROS scavengers were assessed in cell lysates, after 3 h of exposure to 1.0  $\mu$ M A $\beta$ 42 aggregates by a chemiluminescent assay and expressed in ascorbate-equivalent units. The reported values (means  $\pm$  SD) are representative of three independent experiments each carried out in triplicate. \*Significant difference ( $p \leq 0.05$ ) vs relative untreated cells.

E in reducing ROS production induced by A $\beta$  aggregates with respect to relative cells with basal cholesterol content (Fig. 5a). Moreover, the impairment of ROS scavengers was less in cholesterol-enriched FAD cells, matching the almost complete prevention of aggregate-induced oxidative stress obtained by pre-incubating the cells with 100  $\mu$ M vitamin E. Conversely, loss in membrane cholesterol, resulting from cell treatment with  $\beta$ -CD, induced a greater increase in intracellular ROS production and consumption of ROS scavengers (Fig. 5a and b). Notably, PEG-cholesterol and  $\beta$ -CD exposure do not induce ROS production in amyloid untreated fibroblasts, as we can see at time 0 (Fig. 5a).

### 3.3. Membrane cholesterol enrichment reduces A $\beta$ aggregate-induced lipoperoxidation

Membrane lipoperoxidation after aggregate exposure was analyzed by confocal microscopy analysis using the fluorescent probe BODIPY. The red fluorescence observed in basal cholesterol and in  $\beta$ -CD cholesterol-depleted fibroblasts from healthy subjects shifted to green after 3 h of

amyloid aggregate exposure (Fig. 6a). According to previous reported data (Cecchi et al., 2002), PS-1 and, to a greater extent, APP fibroblasts showed a basal oxidative-stressed condition, as revealed by the orange fluorescence in untreated fibroblasts. Anyway, the fluorescence signals observed in membrane cholesterol-enriched cells exposed to A $\beta$ 42 aggregates did not significantly differ from their respective in untreated cells, confirming a fair protective role of membrane cholesterol in FAD cells. Similar experiments carried out in the presence of vitamin E on all investigated fibroblast lines confirmed the specificities of the fluorescence signals. Moreover, we measured the levels of 8-OH isoprostanes, as quantitative lipoperoxidation marker. As shown in Fig. 6b, isoprostanes were significantly higher in APP than in PS-1 fibroblasts, since at a basal level. Cellular isoprostane levels were further increased following A $\beta$ 42 exposure both in cells with basal and, to a greater extent, with reduced membrane cholesterol content. Conversely, membrane cholesterol enrichment was effective in reducing isoprostane production like as vitamin E in FAD fibroblasts treated with A $\beta$ 42 aggregates compared to relative control cells.

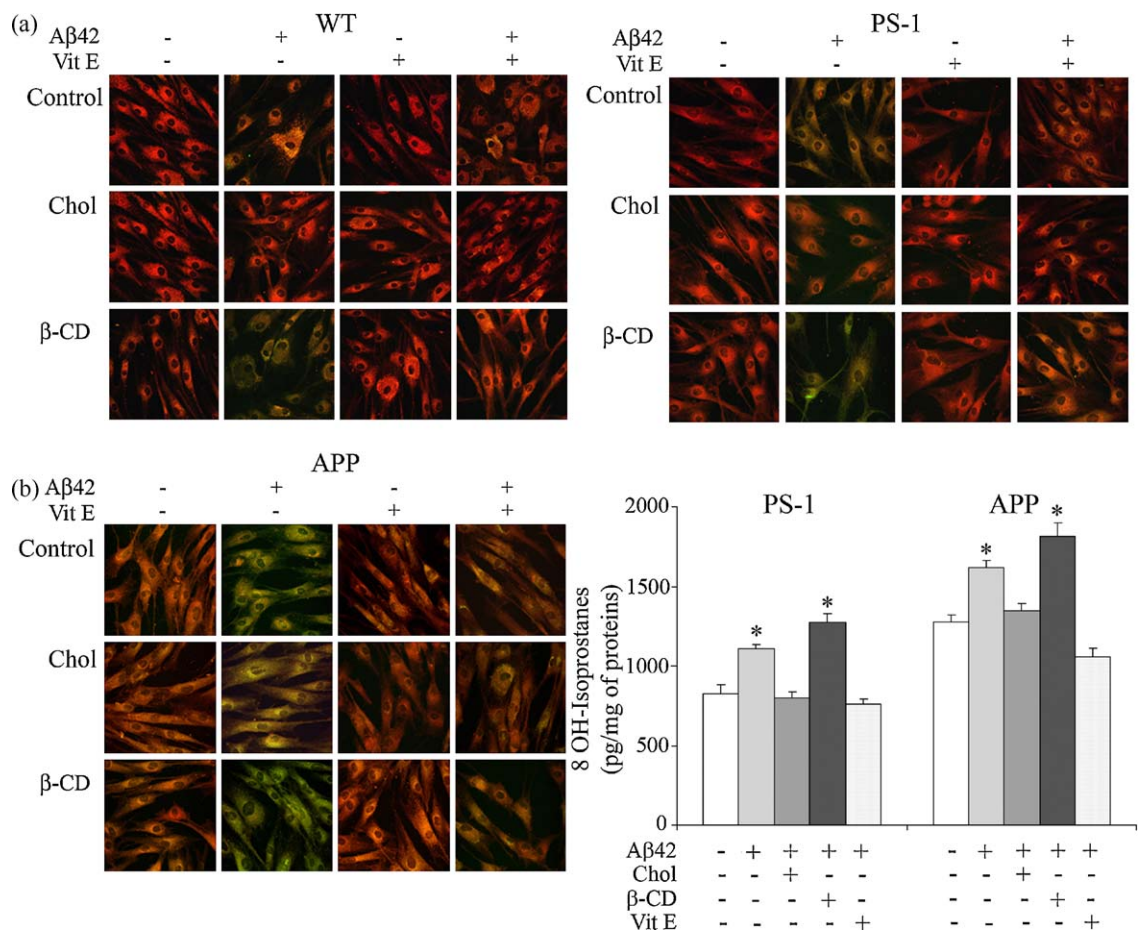


Fig. 6. Cholesterol enrichment protects FAD fibroblasts from Aβ42 peptide-induced lipoperoxidation. (a) Representative confocal microscopy images of lipid peroxidation in WT, PS-1 and APP fibroblasts under different experimental conditions. Cells were treated with 1.0 μM Aβ42 for 3 h, with or without vitamin E (Vit E), and lipid peroxidation was measured using the fluorescent probe BODIPY as a probe according to Section 2. (b) Lipid peroxidation was also measured as cytosolic levels of 8-isoprostanes (for details see Section 2). The reported values (means ± SD) are representative of three independent experiments carried out in triplicate and are expressed as % with respect to untreated cells. \*Significant difference ( $p \leq 0.05$ ) vs relative untreated cells.

### 3.4. High membrane cholesterol prevents Aβ aggregate cytotoxicity

Next we investigated whether changes in oxidative markers also resulted in modulation of Aβ aggregate toxicity to exposed cells. As shown in Fig. 7a, morphological evaluation of healthy and FAD fibroblasts using Hoechst 33342 staining revealed no marked characteristics of apoptosis (i.e. nuclear condensation or DNA fragmentation) in cells enriched in membrane cholesterol after 24 h of exposure to Aβ42 aggregates with respect to similarly exposed control cells with basal cholesterol content. Accordingly, as revealed by the MTT assay (Fig. 7b), both FAD and wild-type fibroblasts with cholesterol-rich membrane were significantly more resistant to Aβ42 aggregate toxicity with respect to similarly exposed control cells with basal cholesterol content. Conversely, loss in membrane cholesterol, following cell treatment with β-CD, resulted in a significant increase in the number of cells showing nuclear condensation, as revealed by the increase in Hoechst fluorescence (Fig. 7a),

and in a significant impairment of cell viability (Fig. 7b) upon exposure to the aggregates. Cell treatment with PEG-cholesterol or β-CD do not affect cell viability (data not shown). Vitamin E and Aβ42-1 reversed sequence peptide were used as negative controls. In particular, the absence of any cytotoxic effect in Aβ42-1 treated cells highlighted the selectivity of the cellular response to Aβ42 peptide aggregates. Moreover, the selectivity of the cytoprotective role of high membrane cholesterol was investigated in cells exposed to different forms of Aβ42 aggregates and to amylin prefibrillar aggregates (Fig. 8). Under our experimental conditions, cholesterol-depleted fibroblasts showed an apparent susceptibility to the Aβ42 mature fibrils, but to a lesser extent than to Aβ42 oligomers. In any case, Aβ42 fibrils induced a more evident DNA damage in APP than in PS1 fibroblasts. On the other hand, cholesterol-enriched fibroblasts displayed no significant change of cell viability upon exposure to Aβ42 fibrils, suggesting that membrane cholesterol enrichment also protects cells from perturbation by fibrillar aggregates. Overall, FAD fibroblasts exposed to fibrils displayed variable

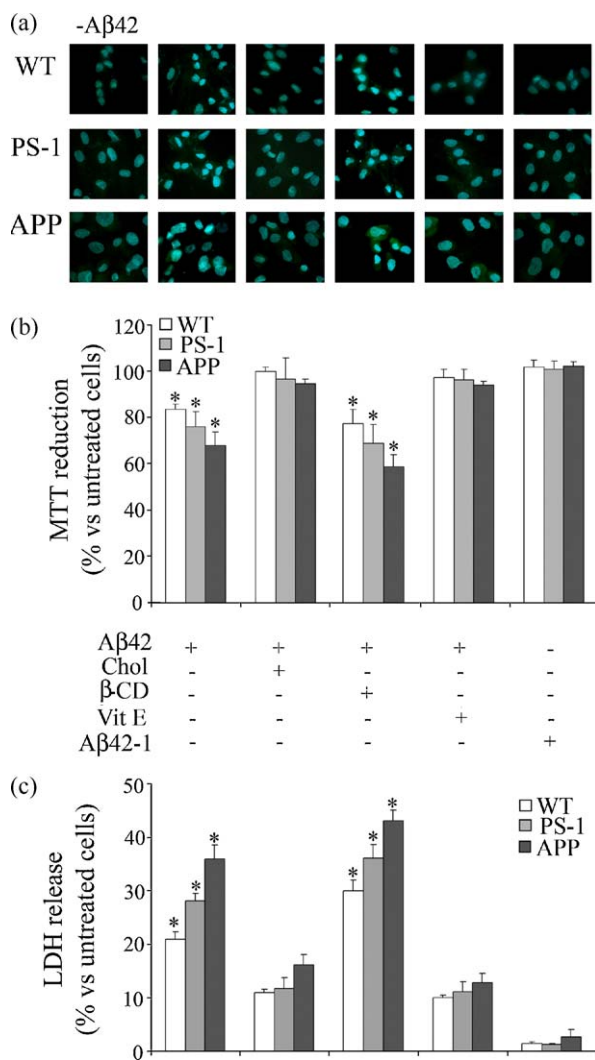


Fig. 7. Cholesterol enrichment prevents A $\beta$  aggregate toxicity. (a) The toxic effect of A $\beta$ 42 aggregates on FAD and healthy fibroblast morphology was evaluated using the Hoechst 33342 dye staining. Representative blue fluorescence micrographs of untreated (–A $\beta$ 42) or exposed fibroblasts to 1.0  $\mu$ M A $\beta$ 42 aggregates for 24 h (for details see Section 2). (b) Cell viability was checked by the MTT reduction test in cells treated with 1.0  $\mu$ M A $\beta$ 42 aggregates for 24 h. The reported values (means  $\pm$  SD) are representative of four independent experiments, each performed in triplicate. (c) Fibroblast viability was checked by LDH release into the culture medium after exposure to 1.0  $\mu$ M A $\beta$ 42 aggregates for 48 h. The values shown are means  $\pm$  SD of three independent experiments, each performed in triplicate. \*Significant difference ( $p \leq 0.05$ ) vs relative untreated cells.

susceptibility to damage and to apoptotic death, confirming a significant inverse relation to membrane content in cholesterol. A reduced vulnerability to the stress induced by amylin oligomers was also observed in cholesterol-enriched fibroblasts with respect to cells with low cholesterol content, further supporting the generality of these effects. On the other hand, a negligible cytotoxicity after treatment with A $\beta$ 42 monomeric peptide further tightly linked previous results to the  $\beta$ -sheet structure found in A $\beta$ 42 and amylin aggregates.

Though displaying the typical features of apoptotic cells, FAD and wild-type fibroblasts with basal and reduced mem-

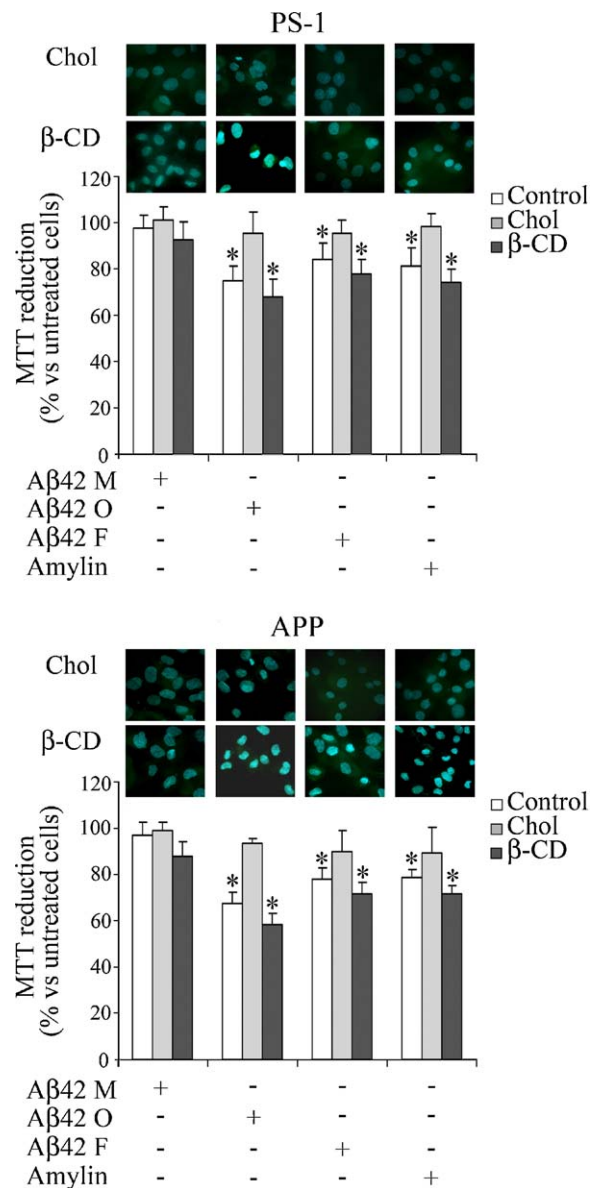


Fig. 8. Cholesterol protects against A $\beta$  fibrils and amylin aggregate toxicity. The toxic effect of 1.0  $\mu$ M A $\beta$ 42 monomers (A $\beta$ 42 M), A $\beta$ 42 oligomers (A $\beta$ 42 O), A $\beta$ 42 fibrils (A $\beta$ 42 F) and amylin aggregates on FAD fibroblasts was evaluated using Hoechst 33342 dye staining. Representative blue fluorescence micrographs of PS-1 and APP fibroblasts exposed to different forms of A $\beta$ 42 or amylin prefibrillar aggregates for 24 h. Cell viability was checked by the MTT reduction test in PS-1 and APP fibroblasts exposed to the same aggregates. The reported values are representative of three independent experiments, each performed in duplicate. \*Significant difference ( $p \leq 0.05$ ) vs relative untreated cells.

brane cholesterol content appeared to be similarly affected by 24 h of A $\beta$ 42 aggregate exposure. Then, we investigated whether fibroblasts exposed to A $\beta$ 42 prefibrillar aggregates for longer times (48 h) underwent a necrotic, rather than apoptotic, cell death. As shown in Fig. 7c, a significant release of LDH in the cell culture media was observed in fibroblasts with basal and, to a greater extent, reduced cholesterol content exposed to A $\beta$  aggregates. Again, cholesterol enriched



fibroblasts displayed a higher resistance to amyloid toxicity, compared to relative control cells, as revealed by the significant reduction of LDH release into the culture media.

#### 4. Discussion

Growing data indicate that changes in membrane cholesterol content, by modulating lipid fluidity, have regulatory consequences for A $\beta$  interactions with the cell plasma membranes and neurotoxicity (Mazziotti and Perlmutter, 1998; Ledesma and Dotti, 2006; Zhou and Richardson, 1996; Yip et al., 2001; Arispe and Doh, 2002; Sponne et al., 2004; Chochina et al., 2001; Cecchi et al., 2008). The present study provides evidence supporting the hypothesis that membrane cholesterol modulation might affect the sensitivity to A $\beta$ 42 aggregates of primary fibroblasts carrying APP Val717Ile or PS-1 Leu392Val or Met146Leu gene mutations by modulating A $\beta$  aggregate binding to the cell membrane, recognized as a primary step in amyloid cytotoxicity. In particular, confocal microscopy images, flow cytometric analysis and Congo red assay revealed that A $\beta$ 42 assemblies accumulate faster, and are internalized to a greater extent into, the plasma membranes of cholesterol-poor fibroblasts than in cholesterol-enriched cells. Indeed, it seems likely that when the level of cholesterol in the membrane is higher than normal, the insertion process can be prevented by the enhanced stiffness of the membrane. On the other hand, when the A $\beta$  oligomer encounters a membrane with increased fluidity due to a lower cholesterol level, the insertion process can occur (Arispe and Doh, 2002). Despite a relatively low number of patient samples employed in our study that limits the statistical power of the results, these findings strongly support the idea that the ability of A $\beta$ 42 aggregates to bind to the plasma membrane is significantly affected by its content in cholesterol (Cecchi et al., 2005). Even in human SH-SY5Y neuroblastoma cells, mild cholesterol enrichment appears to prevent A $\beta$ 42 aggregate binding to the plasma membrane, corroborating our hypothesis in a neuronal system. However, it cannot be excluded that different APP distribution and/or accessibility in the plasma membranes, likely resulting from lipid raft reorganization at the different experimental conditions used, may contribute to the interaction of the A $\beta$  aggregates with the cell membranes. Indeed, recent evidence suggests that A $\beta$  interacts with the APP present at the cell surface and acts as a ligand of its own precursor, resulting in a cell death-related signal (Shaked et al., 2006). Oxidative stress has largely been implicated as a major cause of neurotoxicity in AD and there is strong evidence linking lipid peroxidation and amyloid plaques within the AD brain (Canevari et al., 2004; Lovell and Markesbery, 2006; Subbarao and Richardson, 1990; Squier, 2001; Floyd and Hensley, 2002). Oxidative damage, possibly induced by A $\beta$ , may further exacerbate A $\beta$  toxicity by modulating the A $\beta$  amyloid pathway (Crouch et al., 2007). Indeed, A $\beta$  is reported to accumulate faster in membranes containing

oxidatively damaged phospholipids than in membranes containing only unoxidized or saturated phospholipids (Murray et al., 2007). We have previously shown a marked increase in oxidation levels of lipids and proteins in peripheral cells from some FAD patients (Cecchi et al., 2002). Moreover, we have described that amyloid oligomers can readily insert into oxidative-damaged APPV717I fibroblasts where the membrane integrity is compromised (Cecchi et al., 2007). The early appearance of amyloid aggregates bounded to fibroblast surfaces therefore suggests that these species are the main source of oxidative stress for cells. Actually, cholesterol-poor cells displayed a prompt and enhanced ROS increase upon aggregate binding to the cell membrane with respect to control fibroblasts with basal membrane cholesterol content. Conversely, membrane cholesterol enrichment resulted in a delayed and significantly reduced rise of ROS production in the affected PS-1 and APP fibroblasts exposed to A $\beta$  aggregates. In these cellular models the protective role of membrane cholesterol against amyloid oxidative damage seem particularly hopeful. Our approach allows to study the potential defensive role of a mild membrane cholesterol enrichment against A $\beta$ -induced cytotoxicity in living cells having a genetic drawback in tissues where AD lesions occur. Indeed, mutated fibroblasts displayed a lower level of basal ROS scavengers, thus suggesting that a modified redox status is a common feature of cells carrying these genetic lesions. This evidence could reflect chronic exposure to an oxidizing environment in mutated fibroblasts with a continuous overproduction of amyloid peptide. Several studies provide evidence for excess lipoperoxidation and protein oxidation associated with A $\beta$  deposits in APP and PS-1 AD brain and mutant mice (Butterfield et al., 2007; Canevari et al., 2004). Accordingly, the reported confocal microscopy images and the quantitative analysis of 8-OH isoprostane levels show that A $\beta$ 42 aggregates added to the cell culture media induce a more extensive lipoperoxidation and membrane oxidative injury in APP than in PS-1 mutated fibroblasts. Nevertheless, cholesterol-enriched FAD fibroblasts appear more resistant to amyloid oxidative attack with respect to control cells with basal membrane cholesterol. On the other hand, membrane cholesterol depletion strongly exacerbates A $\beta$ -induced lipid peroxidation. These results therefore suggest that membrane cholesterol content negatively correlates with lipoperoxidant effects on polyunsaturated fatty acids in cell membrane phospholipids induced by A $\beta$ 42 oligomers. Membrane cholesterol enrichment cannot completely revert A $\beta$ 42 oxidative damage in APP mutated fibroblasts, suggesting that other important factors are involved in A $\beta$ 42 aggregate binding to cell membranes. Our previous findings provided compelling evidence that mutated fibroblasts bearing increased membrane lipoperoxidation are more susceptible to aggregate binding to the plasma membrane and to the resulting amyloid toxicity (Cecchi et al., 2007).

This study indicates that membrane cholesterol can readily modulate FAD fibroblasts sensitivity to A $\beta$ -induced



oxidative attack. In particular, membrane cholesterol enrichment resulted in almost complete recovery of mitochondrial function and in a significant reduction of LDH release into the culture media of exposed FAD fibroblasts according to previous data on SH-SY5Y cells, PC12 cells and rat embryo cortical neurons (Yip et al., 2001; Arispe and Doh, 2002; Sponne et al., 2004). On the other hand, cell sensitivity to the cytotoxic effect of A $\beta$ 42 aggregates was significantly enhanced by low cholesterol levels. Remarkably, amylin treatment of low cholesterol fibroblasts affects cell viability resembling A $\beta$ 42 outcome. These data suggest that the modification of membrane cholesterol is generally able to modulate the toxic effect of amyloidogenic peptides independently from their amino acid sequence. Moreover, our data are consistent with increasing evidence that oligomeric aggregates, compared to mature fibrils, are likely the more toxic species of amyloid peptides (Cecchi et al., 2007; Kaye et al., 2004; Klein, 2002; Lacor et al., 2004; Stefani and Dobson, 2003). We can therefore conclude that the presence of  $\beta$ -sheet structure seems to be stringent for the membrane perturbing properties of A $\beta$  oligomers. A moderate, but significant increase of cell resistance to fibril toxicity in fibroblasts with higher membrane cholesterol is likely to be the result of binding inhibition of minute amounts of residual prefibrillar aggregates, although a specific modulation of the toxic effect of the fibrils cannot be ruled out. It has recently been shown that seladin-1 gene, whose proteic product catalyzes the last steps of cholesterol biosynthesis (Waterham et al., 2001), appears to be down-regulated in brain areas affected by AD (Greeve et al., 2000). Our recent findings also indicate that seladin-1-induced membrane cholesterol enrichment protects SH-SY5Y cells against amyloid toxicity by reducing the interaction of A $\beta$ 42 oligomer with cell membrane, featuring seladin-1 as a susceptibility gene candidate for sporadic AD (Cecchi et al., 2008). In this view one might propose that, by modulating the membrane fluidity, plasma membrane cholesterol content may specifically influence APP processing and A $\beta$  production as well as the insertion of soluble A $\beta$  in the phospholipid bilayer and its properties to disturb the membrane structure which ultimately trigger cell death.

## Disclosure statement

(a) All authors disclose any actual or potential conflicts of interest including any financial, personal or other relationships with other people or organizations within three years of beginning the work submitted that could inappropriately influence (bias) their work. No author's institution has contracts relating to this research through which it or any other organization may stand to gain financially now or in the future. There are no other agreements of authors or their institutions that could be seen as involving a financial interest in this work. (b) Appropriate approval and procedures were used concerning human subjects and obtained prior to obtaining

data. The local ethical committee approved the protocol of the study and written consent was obtained from all subjects or, where appropriate, their caregivers.

## Acknowledgements

This study was supported by grants from the Italian MIUR (project numbers 2005054147\_001 and 2005053998\_001).

## References

- Abad-Rodriguez, J., Ledesma, M.D., Craessaerts, K., Perga, S., Medina, M., Delacourte, A., Dingwall, C., De Strooper, B., Dotti, C.G., 2004. Neuronal membrane cholesterol loss enhances amyloid peptide generation. *J. Cell. Biol.* 167, 953–960.
- American Psychiatric Association, 1994. *Diagnostic and Statistical Manual of Mental Disorders*, 4th ed., Washington DC.
- Amundson, D.M., Zhou, M., 1999. Fluorometric method for the enzymatic determination of cholesterol. *J. Biochem. Biophys. Methods* 13 (38), 43–52.
- Arispe, N., Doh, M., 2002. Plasma membrane cholesterol controls the cytotoxicity of Alzheimer's disease A $\beta$ (1–40) and (1–42) peptides. *FASEB J.* 16, 1526–1536.
- Bokvist, M., Lindstrom, F., Watts, A., Grobner, G., 2004. Two types of Alzheimer's beta-amyloid (1–40) peptide membrane interactions: aggregation preventing transmembrane anchoring versus accelerated surface fibril formation. *J. Mol. Biol.* 335, 1039–1049.
- Bradford, M.M., 1976. A rapid and sensitive method for the quantitation of microgram quantities of protein utilizing the principle of protein-dye binding. *Anal. Biochem.* 72, 248–254.
- Butterfield, D.A., Reed, T., Newman, S.F., Sultana, R., 2007. Roles of amyloid beta-peptide-associated oxidative stress and brain protein modifications in the pathogenesis of Alzheimer's disease and mild cognitive impairment. *Free Rad. Biol. Med.* 43, 658–677.
- Canevari, L., Abramov, A.Y., Duchon, M.R., 2004. Toxicity of amyloid beta peptide: tales of calcium, mitochondria, and oxidative stress. *Neurochem. Res.* 29, 637–650.
- Cecchi, C., Fiorillo, C., Sorbi, S., Latorraca, S., Nacmias, B., Bagnoli, S., Nassi, P., Liguri, G., 2002. Oxidative stress and reduced antioxidant defenses in peripheral cells from familial Alzheimer's patients. *Free Rad. Biol. Med.* 33, 1372–1379.
- Cecchi, C., Baglioni, S., Fiorillo, C., Pensalfini, A., Liguri, G., Nosi, D., Rigacci, S., Bucciantini, M., Stefani, M., 2005. Insights into the molecular basis of the differing susceptibility of varying cell types to the toxicity of amyloid aggregates. *J. Cell. Sci.* 118, 3459–3470.
- Cecchi, C., Fiorillo, C., Baglioni, S., Pensalfini, A., Bagnoli, S., Nacmias, B., Sorbi, S., Nosi, D., Relini, A., Liguri, G., 2007. Increased susceptibility to amyloid toxicity in familial Alzheimer's fibroblasts. *Neurobiol. Aging* 28, 863–876.
- Cecchi, C., Rosati, F., Pensalfini, A., Formigli, L., Nosi, D., Liguri, G., Dichiaro, F., Morello, M., Danza, G., Pieraccini, G., Peri, A., Serio, M., Stefani, M., 2008. Seladin-1/DHCR24 protects neuroblastoma cells against A $\beta$  toxicity by increasing membrane cholesterol content. *J. Cell. Mol. Med.* 12, 1990–2002.
- Chochina, S.V., Avdulov, N.A., Igbavboa, U., Cleary, J.P., O'Hare, E.O., Wood, W.G., 2001. Amyloid beta-peptide 1–40 increases neuronal membrane fluidity: role of cholesterol and brain region. *J. Lipid Res.* 42, 1292–1297.
- Citron, M., Westaway, D., Xia, W., Carlson, G., Diehl, T., Levesque, G., Johnson-Wood, K., Lee, M., Seubert, P., Davis, A., Kholodenko, D., Motter, R., Sherrington, R., Perry, B., Yao, H., Strome, R., Lieberburg, I., Rommens, J., Kim, S., Schenk, D., Fraser, P., St George Hyslop, P., Selkoe, D.J., 1997. Mutant presenilins of Alzheimer's disease increase

- production of 42-residue amyloid beta-protein in both transfected cells and transgenic mice. *Nat. Med.* 3, 67–72.
- Crouch, P.J., Harding, S.M.E., White, A.R., Camakaris, J., Bush, A.I., Masters, C.L., 2007. Mechanisms of A $\beta$  mediated neurodegeneration in Alzheimer's disease. *Int. J. Biochem. Cell. Biol.* 40, 181–198.
- Cruts, M., Van Broeckoven, C., 1998. Molecular genetics of Alzheimer's disease. *Ann. Med.* 30, 560–565.
- Dahlgren, K.N., Manelli, A.M., Stine, W.B., Baker, L.K., Krafft, G.A., LaDu, M.J., 2002. Oligomeric and Fibrillar species of amyloid- $\beta$  peptides differentially affect neuronal viability. *J. Biol. Chem.* 277, 32046–32053.
- Datki, Z., Papp, R., Zadori, D., Soos, K., Fulop, L., Juhasz, A., Laskay, G., Hetenyi, C., Mihalik, E., Zarandi, M., Penke, B., 2004. In vitro model of neurotoxicity of Abeta 1–42 and neuroprotection by a pentapeptide: irreversible events during the first hour. *Neurobiol. Dis.* 17, 507–515.
- Drummen, G.P.C., Gadella, B.M., Post, J.A., Brouwers, J.F., 2004. Mass spectrometric characterization of the oxidation of the fluorescent lipid peroxidation reporter molecule C11-BODIPY581/591. *Free Rad. Biol. Med.* 36, 1635–1644.
- Floyd, R.A., Hensley, K., 2002. Oxidative stress in brain aging. Implications for therapeutics of neurodegenerative diseases. *Neurobiol. Aging* 23, 795–807.
- Greeve, I., Hermans-Borgmeyer, I., Brellinger, C., Kasper, D., Gomez-Isla, T., Behl, C., Levkau, B., Nitsch, R.M., 2000. The human DIMINUTO/DWARF1 homolog seladin-1 confers resistance to Alzheimer's disease-associated neurodegeneration and oxidative stress. *J. Neurosci.* 20, 7345–7352.
- Kawahara, M., Kuroda, Y., 2001. Intracellular calcium changes in neuronal cells induced by Alzheimer's beta-amyloid protein are blocked by estradiol and cholesterol. *Cell. Mol. Neurobiol.* 21, 1–13.
- Kayed, R., Sokolov, Y., Edmonds, B., McIntire, T.M., Milton, S.C., Hall, J.E., Glabe, C.G., 2004. Permeabilization of lipid bilayers is a common conformation-dependent activity of soluble amyloid oligomers in protein misfolding diseases. *J. Biol. Chem.* 279, 46363–46366.
- Klein, W.L., 2002. A $\beta$  toxicity in Alzheimer's disease: globular oligomers (ADDLs) as new vaccine and drug targets. *Neurochem. Int.* 41, 345–352.
- Lacor, P.N., Buniel, M.C., Chang, L., Fernandez, S.J., Gong, Y., Viola, K.L., Lambert, M.P., Velasco, P.T., Bigio, E.H., Finch, C.E., Krafft, G.A., Klein, W.I., 2004. Synaptic targeting by Alzheimer's-related amyloid  $\beta$  oligomers. *J. Neurosci.* 24, 10191–10200.
- Lambert, M.P., Viola, K.L., Chromy, B.A., Chang, L., Morgan, T.E., Yu, J., Venton, D.L., Krafft, G.A., Finch, C.E., Klein, W.L., 2001. Vaccination with soluble A $\beta$  oligomers generates toxicity-neutralizing antibodies. *J. Neurochem.* 79, 595–605.
- Ledesma, M.D., Dotti, C.G., 2006. Amyloid excess in Alzheimer's disease: what is cholesterol to be blamed for? *FEBS Lett.* 580, 5525–5532.
- Lin, M.C., Kagan, B., 2002. Electrophysiologic properties of channels induced by A $\beta$ 25–35 in planar lipid bilayers. *Peptides* 23, 1215–1228.
- Lovell, M.A., Markesbery, W.R., 2006. Amyloid beta peptide, 4-hydroxynonenal and apoptosis. *Curr. Alzheimer Res.* 3, 359–364.
- Mazziotti, M., Perlmutter, D.H., 1998. Resistance to the apoptotic effect of aggregated amyloid- $\beta$  peptide in several different cell types including neuronal- and hepatoma-derived cell lines. *Biochem. J.* 332, 517–524.
- Mirzabekov, T.A., Lin, M.C., Kagan, B., 1996. Pore formation by the cytoxic islet amyloid peptide amylin. *J. Biol. Chem.* 271, 1988–1992.
- Murray, I.V., Liu, L., Komatsu, H., Uryu, K., Xiao, G., Lawson, J.A., Axelsen, P.H., 2007. Membrane-mediated amyloidogenesis and the promotion of oxidative lipid damage by amyloid beta proteins. *J. Biol. Chem.* 282, 9335–9345.
- Naguib, Y.M., 1998. A fluorometric method for measurement of peroxyl radical scavenging activities of lipophilic antioxidants. *Anal. Biochem.* 265, 290–298.
- Pensalfini, A., Cecchi, C., Zampagni, M., Becatti, M., Favilli, F., Paoli, P., Catarzi, S., Bagnoli, S., Nacmias, B., Sorbi, S., Liguri, G., 2008. Protective effect of new S-acyl-glutathione derivatives against amyloid-induced oxidative stress. *Free Rad. Biol. Med.* 44 (8), 1624–1636.
- Selkoe, D.J., 2001. Alzheimer's disease: genes, proteins, and therapy. *Physiol. Rev.* 81, 741–766.
- Shaked, G.M., Kummer, M.P., Lu, D.C., Galvan, V., Bredesen, D.E., Koo, E.H., 2006. Abeta induces cell death by direct interaction with its cognate extracellular domain on APP (APP 597–624). *FASEB J.* 20, 1254–1256.
- Simakova, O., Arispe, N.J., 2007. The cell-selective neurotoxicity of the Alzheimer's Abeta peptide is determined by surface phosphatidylserine and cytosolic ATP levels. Membrane binding is required for Abeta toxicity. *J. Neurosci.* 27, 13719–13729.
- Sponne, I., Fifre, A., Koziel, V., Oster, T., Olivier, J.L., Pillot, T., 2004. Membrane cholesterol interferes with neuronal apoptosis induced by soluble oligomers but not fibrils of the amyloid  $\beta$  peptide. *FASEB J.* 18, 836–838.
- Squier, T.C., 2001. Oxidative stress and protein aggregation during biological aging. *Exp. Gerontol.* 36, 1539–1550.
- Stefani, M., Dobson, C.M., 2003. Protein aggregation and aggregate toxicity: new insights into protein folding, misfolding diseases and biological evolution. *J. Mol. Med.* 81, 678–699.
- Subbarao, K.V., Richardson, J.S., 1990. Autopsy samples of Alzheimer's cortex show increased peroxidation in vitro. *J. Neurochem.* 55, 342–345.
- Tabaton, M., Tamagno, E., 2007. The molecular link between beta- and gamma-secretase activity on the amyloid beta precursor protein. *Cell. Mol. Life Sci.* 64, 2211–2218.
- Takeda, K., Araki, W., Tabira, T., 2004. Enhanced generation of intracellular Abeta42 amyloid peptide by mutation of presenilins PS1 and PS2. *Eur. J. Neurosci.* 19, 258–264.
- The Dementia Study Group of the Italian Neurological Society, 2000. Guidelines for the diagnosis of dementia and Alzheimer's disease. *Ital. J. Neurol. Sci.* 21, 87–194.
- Wakabayashi, M., Okada, T., Kozutsumi, Y., Matsuzaki, K., 2005. GM1 ganglioside-mediated accumulation of amyloid beta-protein on cell membranes. *Biochim. Biophys. Res. Commun.* 328, 1019–1023.
- Waterham, H.R., Koster, J., Romeijn, G.J., Hennekam, R.C., Vreken, P., Andersson, H.C., FitzPatrick, D.R., Kelley, R.I., Wanders, R.J., 2001. Mutations in the 3 $\beta$ -hydroxysterol  $\Delta$ 24 reductase gene cause desmosterolosis, an autosomal recessive disorder of cholesterol biosynthesis. *Am. J. Hum. Genet.* 69, 685–694.
- Yip, C.M., Elton, E.A., Darabie, A.A., Morrison, M.R., McLaurin, J., 2001. Cholesterol, a modulator of membrane-associated Abeta-fibrillogenesis and neurotoxicity. *J. Mol. Biol.* 311, 723–734.
- Zhou, Y., Richardson, J.S., 1996. Cholesterol protects PC12 cells from beta-amyloid induced calcium disordering and cytotoxicity. *Neuroreport* 7, 2487–2490.